Self-Assembly of Cationic Pd(II)/Pt(II) Metallomacrocycles Containing Tetrahedral C_2Co_2 Clusters from Rigid Cluster-Bridged Bipyridine $(4\text{-}C_5H_4N)_2C_2Co_2(CO)_6$ and Diphosphine- or Diarsine-Chelated Pd(II)/Pt(II) Complexes $[M(dppb)(H_2O)_2][OTf]_2$ (M = Pd, Pt), $[Pd(dpab)(H_2O)(OTf)][OTf]$, and $[Pt(dpab)(H_2O)_2][OTf]_2$

Li-Cheng Song,* Guo-Xia Jin, Hu-Ting Wang, Wen-Xiong Zhang, and Qing-Mei Hu

Department of Chemistry, State Key Laboratory of Elemento-Organic Chemistry, Nankai University, Tianjin 300071, China

Received August 3, 2005

The preparation, characterization, and some properties of the C_2Co_2 cluster-bridged bipyridine ligand $(4\text{-}C_5H_4N)_2C_2Co_2(CO)_6$ (**1**), diphosphine-chelated Pd(II)/Pt(II) complexes $[M(dppb)(H_2O)_2][OTf]_2$ (dppb = 1,4-bis(diphenylphosphino)butane, OTf = SO_3CF_3; **2**, M = Pd; **3**, M = Pt), and the unique cationic cluster-containing Pd(II)/Pt(II) macrocycles $\{[M(dppb)]\text{-}\mu\text{-}[(4\text{-}C_5H_4N)_2C_2Co_2(CO)_6]\}_2[OTf]_4$ (**4**, M = Pd; **5**, M = Pt) and $\{[M(dpab)]\text{-}\mu\text{-}[(4\text{-}C_5H_4N)_2C_2Co_2(CO)_6]\}_2[OTf]_4$ (dpab = 1,4-bis(diphenylarsino)butane; **6**, M = Pd; **7**, M = Pt) are reported. While ligand **1** is prepared by reaction of bis(4-pyridyl)acetylene with $Co_2(CO)_8$ in 61% yield, complexes **2** and **3** are prepared by reaction of $M(dppb)Cl_2$ with silver triflate followed by hydrolysis of the intermediates $M(dppb)(OTf)_2$ in 96% and 94% yields, respectively. Particularly interesting is that the self-assembly of ligand **1** with **2** and **3** results in formation of the C_2Co_2 cluster-containing macrocycles **4** and **5** in 62% and 65% yields, whereas **6** and **7** can be produced by self-assembly of **1** with diarsine-chelated complexes $[Pd(dpab)(H_2O)(OTf)][OTf]$ and $[Pt(dpab)(H_2O)_2][OTf]_2$ in 79% and 68% yields, respectively. **1**−**7** have been fully characterized by elemental analysis, spectroscopy, and particularly for **2**−**7** X-ray crystallography, and for **1**, **4**, and **7** by cyclic voltammetric techniques.

Introduction

Transition metal-directed self-assembly is a widely used synthetic methodology and has played an important role in the development of supramolecular chemistry in recent years.[1−3] So far, a great variety of metallomacrocyclic compounds, such as molecular squares,[4] rectangles,[5] parallelograms,[6] and rhomboids,[7] have been synthesized by self-assembly via dative bonding of nitrogen-containing ligands with transition metal complexes. Recently, we reported two novel metallomacrocycles that were prepared by self-assembly of a flexible C_2Co_2 cluster-bridged bipyridine ligand $(4\text{-}C_5H_4NCO_2CH_2)_2C_2Co_2(CO)_6$ with diarsine-chelated Pd(II)/Pt(II) complexes $[Pd(dpab)(H_2O)(OTf)][OTf]$ and $[Pt(dpab)(H_2O)_2[OTf]_2$ (dpab = 1,4-bis(diphenylarsino)-butane; OTf = SO_3CF_3).[8] As a continuation of this project, we now report the self-assembly of a rigid C_2Co_2

* To whom correspondence should be addressed. Fax: 0086-22-23504853. E-mail: lcsong@nankai.edu.cn.

(1) Vögtle, F. *Supramolecular Chemistry, An Introduction*; Wiley: Chichester, 1991.

(2) Lehn, J.-M. *Supramolecular Chemistry*; *Concepts and Perspectives*; VCH: New York, 1995.

(3) For recent reviews, see: (a) Leininger, S.; Olenyuk, B.; Stang, P. J. *Chem. Rev*. **2000**, *100*, 853.(b) Holliday, B. J.; Mirkin, C. A. *Angew. Chem. Int. Ed.* **2001**, *40*, 2022. (c) Fujita, M.; Umemoto, K.; Yoshizawa, M.; Fujita, N.; Kusukawa, T.; Biradha, K. *Chem. Commun*. **2001**, 509. (d) Swiegers, G. F.; Malefetse, T. J. *Chem. Rev*. **2000**, *100*, 3483. (e) Sun, S.-S.; Lees, A. J. *Coord. Chem. Rev*. **2002**, *230*, 171. (f) Cotton, F. A.; Lin, C.; Murillo, C. A. *Acc. Chem. Res*. **2001**, *10*, 34. (g) MacGillivray, L. R.; Atwood, J. L. *Angew. Chem. Int. Ed*. **1999**, *38*, 1018.

(4) (a) Stang, P. J.; Cao, D. H.; Saito, S.; Arif, A. M. *J. Am. Chem. Soc.* **1995**, *117*, 6273. (b) Stang, P. J.; Olenyuk, B.; Fan, J.; Arif, A. M. *Organometallics* **1996**, *15*, 904. (c) Fujita, M.; Yu, S.-Y.; Kusukawa, T.; Funaki, H.; Ogura, K.; Yamaguchi, K. *Angew. Chem. Int. Ed.* **1998**, *37*, 2082. (d) Stang, P. J.; Cao, D. H. *J. Am. Chem. Soc*. **1994**, *116*, 4981. (e) Fujita, M.; Kwon, Y. J.; Washizu, S.; Ogura, K. *J. Am. Chem. Soc*. **1994**, *116*, 1151. (f) Rauter, H.; Hillgeris, E. C.; Erxleben, A.; Lippert, B. *J. Am. Chem. Soc*. **1994**, *116*, 616. (g) Davies, S. C.; Duhme, A.-K.; Hughes, D. L. *Inorg. Chem*. **1998**, *37*, 5380. (h) Fujita, M.; Yazaki, J.; Ogura, K. *J. Am. Chem. Soc*. **1990**, *112*, 5645. (i) Stang, P. J.; Chen, K.; Arif, A. M. *J. Am. Chem. Soc*. **1995**, *117*, 8793. (j) Stang, P. J.; Chen, K. *J. Am. Chem. Soc*. **1995**, *117*, 1667.

(5) (a) Jeong, K.-S.; Cho, Y. L.; Song, J. U.; Chang, H.-Y.; Choi, M.-G. *J. Am. Chem. Soc*. **1998**, *120*, 10982. (b) Fujita, M. *Chem. Soc. Rev*. **1998**, *27*, 417. (c) Woessner, S. M.; Helms, J. B.; Shen, Y.; Sullivan, B. P. *Inorg. Chem*. **1998**, *37*, 5406. (d) Benkstein, K. D.; Hupp, J. T.; Stern, C. L. *Inorg. Chem*. **1998**, *37*, 5404. (e) Benkstein, K. D.; Hupp, J. T.; Stern, C. L. *J. Am. Chem. Soc*. **1998**, *120*, 12982.

(6) (a) Habicher, T.; Nierengarten, J.-F.; Gramlich, V.; Diederich, F. *Angew. Chem. Int. Ed.* **1998**, *37*, 1916. (b) Fujita, M.; Aoyagi, M.; Ogura, K. *Inorg. Chim. Acta* **1996**, *246*, 53. (c) Hartshorn, C. M.; Steel, P. J. *Inorg. Chem*. **1996**, *35*, 6902.

(7) (a) Schmitz, M.; Leininger, S.; Fan, J.; Arif, A. M.; Stang, P. J. *Organometallics* **1999**, *18*, 4817. (b) Mukherjee, P. S.; Das, N.; Kryschenko, Y. K.; Arif, A. M.; Stang, P. J. *J. Am. Chem. Soc.* **2004**, *126*, 2464. (c) Tabellion, F. M.; Seidel, S. R.; Arif, A. M.; Stang, P. J. *J. Am. Chem. Soc.* **2001**, *123*, 7740.

(8) Song, L.-C.; Jin, G.-X.; Zhang, W.-X.; Hu, Q.-M. *Organometallics* **2005**, *24*, 700.

10.1021/om050668s CCC: $30.25
Publication on Web 11/04/2005

Scheme 1

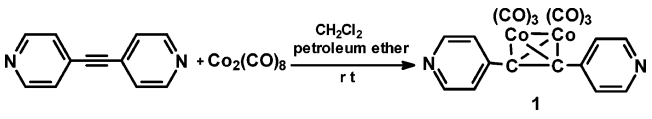

Scheme 2

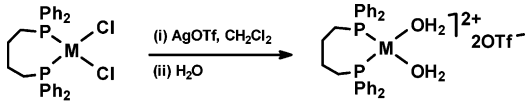

cluster-bridged bipyridine ligand $(4\text{-}C_5H_4N)_2C_2Co_2(CO)_6$ with diphosphine-chelated Pd(II)/Pt(II) complexes $[M(dppb)(H_2O)_2][OTf]_2$ (dppb = 1,4-bis(diphenylphosphino)butane) or with diarsine-chelated Pd(II)/Pt(II) complexes [Pd(dpab)(H_2O)(OTf)][OTf] and [Pt(dpab)-$(H_2O)_2][OTf]_2$. Interestingly, as can be seen in this paper, four new tetrahedral C_2Co_2 cluster-containing metallomacrocycles that have unique structures and interesting properties have been synthesized through such self-assembly reactions. In addition, the synthesis of the new ligand $(4\text{-}C_5H_4N)_2C_2Co_2(CO)_6$ and new starting Pd(II)/Pt(II) complexes $[M(dppb)(H_2O)_2][OTf]_2$ along with their characterization and some properties are also described.

Results and Discussion

Synthesis and Characterization of Tetrahedral C_2Co_2 Cluster-Bridged Bipyridine Ligand $(4\text{-}C_5H_4N)_2C_2Co_2(CO)_6$ (1). We found that treatment of bis(4-pyridyl)acetylene with $Co_2(CO)_8$ in CH_2Cl_2/petroleum ether at room temperature for 2−3 h gave rise to the tetrahedral C_2Co_2 cluster-bridged bipyridine **1** in 61% yield (Scheme 1). Ligand **1** is a rigid bipyridine derivative that contains a tetrahedral C_2Co_2 cluster core directly attached to two pyridine rings. This rigid C_2Co_2 cluster-bridged bipyridine (similar to its flexible analogue $(4\text{-}C_5H_4NCO_2CH_2)_2C_2Co_2(CO)_6$)[8] has been proved to be a very effective bidentate ligand for self-assembly of the tetrahedral C_2Co_2 cluster-containing metallomacrocycles (vide infra). Ligand **1** has been characterized by elemental analysis, IR, ^{1}H NMR, and ^{13}C NMR spectroscopy, which coincide very well with its structure. For example, the IR spectrum of **1** showed five strong absorption bands in the range 2093−2004 cm^{-1} for its terminal carbonyls, whereas the ^{1}H NMR spectrum displayed two doublets at 8.60 and 7.34 ppm for hydrogen atoms in its pyridyl groups and the ^{13}C NMR spectrum exhibited the corresponding signals for carbon atoms present in its terminal carbonyls, pyridine rings, and the C_2Co_2 cluster core, respectively.

Synthesis and Characterization of Diphosphine-Chelated Pd(II)/Pt(II) Complexes $[M(dppb)(H_2O)_2][OTf]_2$ (2, M = Pd; 3, M = Pt). We further found that dppb-chelated Pd(II)/Pt(II) dichlorides $M(dppb)Cl_2$ reacted with silver triflate in CH_2Cl_2 at room temperature for 24 h, followed by treatment of the resulting mixture in air, to afford the corresponding diphosphine dppb-chelated complexes **2** and **3** in 96% and 94% yields (Scheme 2). Apparently, it is believed that reaction of $M(dppb)Cl_2$ with silver triflate might first give bis(triflate) complexes $M(dppb)(OTf)_2$,[9] and diaqua complexes **2** and **3** were finally produced by hydrolysis of the intermediates $M(dppb)(OTf)_2$ in the open air workup process.[4a,b,8] Complexes **2** and **3** have been fully characterized by elemental analysis, spectroscopy, and X-ray diffraction analysis. For instance, the IR spectra of **2** and **3** displayed a broad absorption band at 3221 or 3056 cm^{-1} for their coordinated water, and the ^{19}F NMR spectra of **2** and **3** exhibited one singlet at ca. −79 ppm for their two uncoordinated OTf groups. In addition, while the ^{31}P NMR spectrum of **2** showed one singlet at 35.18 ppm for its two identical P atoms, the spectrum of **3** displayed one triplet at 10.47 ppm (due to the ^{195}Pt−^{31}P coupling) for its two identical P atoms.

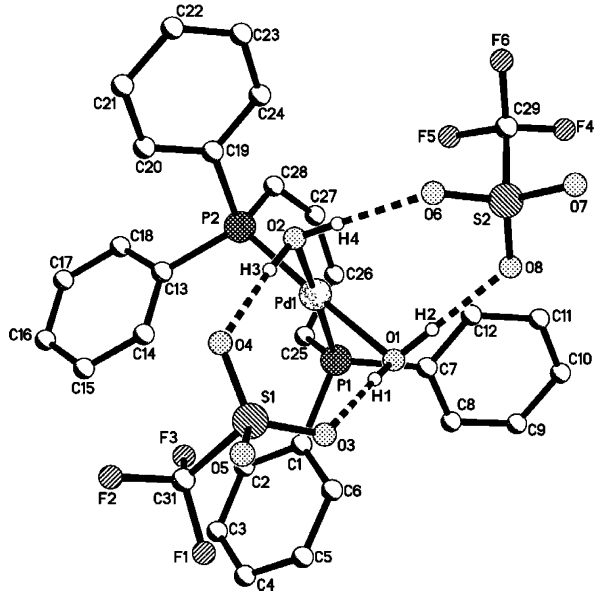

Figure 1. Molecular structure of complex **2**.

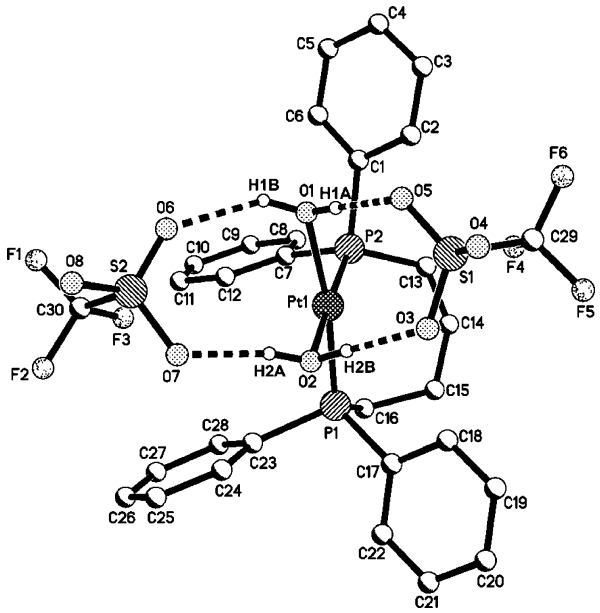

Figure 2. Molecular structure of complex **3**.

The molecular structures of **2** and **3** were unequivocally confirmed by crystal X-ray diffraction analysis. Figures 1 and 2 show their molecular structures, whereas selected bond lengths and angles are listed in

(9) Pignat, K.; Vallotto, J.; Pinna, F.; Strukul, G. *Organometallics* **2000**, *19*, 5160.

Table 1. Selected Bond Lengths (Å) and Angles (deg) for 2

Pd(1)-O(2)	2.150(4)	P(1)−C(7)	1.819(5)
Pd(1)−O(1)	2.155(4)	P(1)−C(25)	1.822(6)
Pd(1)−P(1)	2.2516(16)	S(1)−O(3)	1.436(5)
Pd(1)−P(2)	2.2564(17)	S(1)−C(31)	1.817(7)
P(1)−C(1)	1.813(6)	F(1)−C(31)	1.313(8)
O(2)−Pd(1)−O(1)	86.27(16)	O(3)−S(1)−O(4)	113.6(3)
O(2)−Pd(1)−P(1)	172.44(14)	O(3)−S(1)−C(31)	104.2(4)
O(1)−Pd(1)−P(1)	87.83(11)	F(1)−C(31)−S(1)	111.8(5)
O(2)−Pd(1)−P(2)	92.95(13)	C(6)−C(1)−C(2)	118.6(6)
O(1)−Pd(1)−P(2)	178.31(12)	C(1)−P(1)−C(7)	108.3(3)
P(1)−Pd(1)−P(2)	93.07(6)	C(1)−P(1)−C(25)	105.7(3)

Table 2. Selected Bond Lengths (Å) and Angles (deg) for 3

Pt(1)−O(2)	2.118(4)	P(2)−C(7)	1.805(7)
Pt(1)−O(1)	2.134(5)	P(2)−C(13)	1.825(9)
Pt(1)−P(1)	2.2211(18)	S(1)−O(3)	1.435(6)
Pt(1)−P(2)	2.2197(19)	S(1)−C(29)	1.777(10)
P(2)−C(1)	1.818(8)	F(4)−C(29)	1.319(14)
O(2)−Pt(1)−O(1)	84.72(19)	O(3)−S(1)−O(4)	113.3(4)
O(2)−Pt(1)−P(1)	87.32(12)	O(3)−S(1)−C(29)	103.3(6)
O(1)−Pt(1)−P(1)	169.99(17)	F(4)−C(29)−S(1)	109.3(8)
O(2)−Pt(1)−P(2)	176.35(12)	C(1)−C(2)−C(3)	122.5(10)
O(1)−Pt(1)−P(2)	93.26(16)	C(1)−P(2)−C(7)	106.1(3)
P(1)−Pt(1)−P(2)	95.01(7)	C(1)−P(2)−C(13)	101.4(5)

Tables 1 and 2, respectively. As shown in Figure 1, complex **2** contains one cation, $[Pd(dppb)(H_2O)_2]^{2+}$, in which the transition metal palladium, namely, Pd(1), is ligated to two molecules of water through O(1) and O(2) and one molecule of dppb through P(1) and P(2). In addition, the bond angle around Pd(1) is exactly 360°, which means that Pd(1) adopts a square-planar coordination geometry. The complex cation $[Pd(dppb)(H_2O)_2]^{2+}$ is interacted with two uncoordinated $[OTf]^-$ anions through one type of four intramolecular hydrogen bonds[10] formed by the two coordinated water in the complex cation and the two uncoordinated $[OTf]^-$ anions. The bond lengths of these hydrogen bonds are O(1)−H(1)···O(3) = 2.685 Å, O(1)−H(2)···O(8) = 2.721 Å, O(2)−H(3)···O(4) = 2.740 Å, and O(2)−H(4)···O(6) = 2.748 Å, while the bond angles of these hydrogen bonds are 167.51°, 178.22°, 175.94°, and 173.74°, respectively. Complex **3** (Figure 2) is actually isostructural with complex **2**. For example, the sum of bond angles around Pt(1) is also 360°, and thus its coordination geometry is square-planar. In addition, it also has the same type of four intramolecular hydrogen bonds; the bond lengths of these hydrogen bonds are O(1)−H(1A)···O(5) = 2.701 Å, O(1)−H(1B)···O(6) = 2.826 Å, O(2)−H(2A)···O(7) = 2.602 Å, and O(2)−H(2B)···O(3) = 2.641 Å, whereas the corresponding bond angles are 176.4°, 145°, 168.6°, and 177°, respectively.

It is worth pointing out that the intramolecular hydrogen bonding in the solid state of **2** and **3** is very similar to that of the dpab-chelated Pt(II) complex $[Pt(dpab)(H_2O)_2][OTf]_2$, but is quite different from that of the dpab-chelated Pd(II) complex $[Pd(dpab)(H_2O)(OTf)][OTf]$. In addition, it is due to the presence of intramolecular hydrogen bonding in diaqua complexes **2** and **3** that the air and thermal stability of **2** and **3** is much higher than their precursors of the bis(triflate) complexes $M(dppb)(OTf)_2$. In fact, the function of hydrogen bonding in the stabilization of the solid-state structure of aqua-transition metal complexes has been well documented.[10,11]

Synthesis and Characterization of Tetrahedral C_2Co_2 Cluster-Containing Macrocycles $\{[M(dppb)]$-μ-$[(4\text{-}C_5H_4N)_2C_2Co_2(CO)_6]\}_2[OTf]_4$ (4, M = Pd, ; 5, M = Pt) and $\{[M(dpab)]$-μ-$[(4\text{-}C_5H_4N)_2C_2Co_2(CO)_6]\}_2[OTf]_4$ (6, M = Pd; 7, M = Pt). Interestingly, the C_2Co_2 cluster-bridged bipyridine **1** reacted with dppb-chelated complexes $[M(dppb)(H_2O)_2][OTf]_2$ (**2**, M = Pd; **3**, M = Pt) in CH_2Cl_2 at room temperature for 1−2 h to give the C_2Co_2 cluster-containing macrocycles **4** and **5** in 62% and 65% yields, while it was treated with dpab-chelated complexes $[Pd(dpab)(H_2O)(OTf)][OTf]$ and $[Pt(dpab)(H_2O)_2][OTf]_2$ under similar conditions to produce the corresponding macrocyclic compounds **6** and **7** in 79% and 68% yields, respectively (Scheme 3).

Products **4**−**7** have been fully characterized by elemental analysis, spectroscopy, and X-ray crystallography. The IR spectra of **4**−**7** displayed three strong absorption bands in the range 2105−2044 cm^{-1} for their terminal carbonyls, which are in higher frequencies in comparison with those displayed by the terminal carbonyls of free ligand **1**. This is obviously due to ligand **1** being located in the cationic $\{[M(dppb)]$-μ-$[(4\text{-}C_5H_4N)_2C_2Co_2(CO)_6]\}_2^{4+}$ and $\{[M(dpab)]$-μ-$[(4\text{-}C_5H_4N)_2C_2Co_2(CO)_6]\}_2^{4+}$ macrocycles.[12] In addition, as compared with those of starting complexes **2** and **3**, the ^{31}P NMR signals of **4** and **5** were shown to be shifted to higher field, which could be attributed to the original positive charges centered at Pd/Pt atoms of **2** and **3** being dispersed in the conjugated cationic macrocycles of **4** and **5**. The presence of triflate ions in **4**−**7** is indicated by one singlet in their ^{19}F NMR spectra at about −78.7 ppm. Thus, the ^{19}F NMR behavior of the triflates in macrocycles **4**−**7** is very close to that of the triflates in their precursors and the other Pd(II)/Pt(II) complexes.[4a,b,8]

Fortunately, the molecular structures of **4**−**7** have been unambiguously confirmed by X-ray diffraction techniques. The ORTEP diagrams of cationic portions of **4**−**7** are shown in Figures 3−6, whereas selected bond lengths and angles are given in Tables 3−6, respectively. As shown in Figures 3−6, the macrocyclic cations of **4**−**7** are centrosymmetric and are composed of two dppb- or dpab-chelated transition metal Pd or Pt units, which are combined together via two tetrahedral C_2Co_2 cluster-bridged bipyridine ligands. The coordination geometry around the palladium or platinum atoms in **4**−**7** is square-planar with some deviations of the bond angles from ideal 90°. In **4** and **5** the angles P−Pd−P, P−Pt−P, N−Pd−N, and N−Pt−N are 95.68(7)°, 97.02(9)°, 86.1(2)°, and 85.7(2)°, whereas in **6** and **7** the angles As−Pd−As, As−Pt−As, N−Pd−N, and N−Pt−N are 94.28(4)°, 95.15(4)°, 87.5(2)°, and 87.8(3)°, respectively. While the nonbonded Pd···Pd and Pt···Pt distances in **4** and **5** are 10.813 and 10.773 Å, the Pd···Pd and Pt···Pt distances in **6** and **7** are 10.732 and 10.637 Å, respectively.

(10) Kollman, P. A.; Allen, L. C. *Chem. Rev.* **1972**, *72*, 283.

(11) See, for example: (a) Rochon, F. D.; Melanson, R. *Inorg. Chem.* **1987**, *26*, 989. (b) Britten, J. F.; Lippert, B.; Lock, C. J. L.; Pilon, P. *Inorg. Chem*. **1982**, *21*, 1936. (c) Hollis, L. S.; Lippard, S. J. *Inorg. Chem.* **1983**, *22*, 2605. (d) Braga, D.; Grepioni, F. *Acc. Chem. Res.* **1994**, *27*, 51. (e) Braga, D.; Grepioni, F.; Sabatino, P.; Desiraju, G. R. *Organometallics* **1994**, *13*, 3532.

(12) Collman, J. P.; Hegedus, L. S.; Norton, J. R.; Finke, R. G. *Principles and Applications of Organotransition Metal Chemistry*, 2nd ed.; California University Science Books: Mill Valley, 1987.

Scheme 3

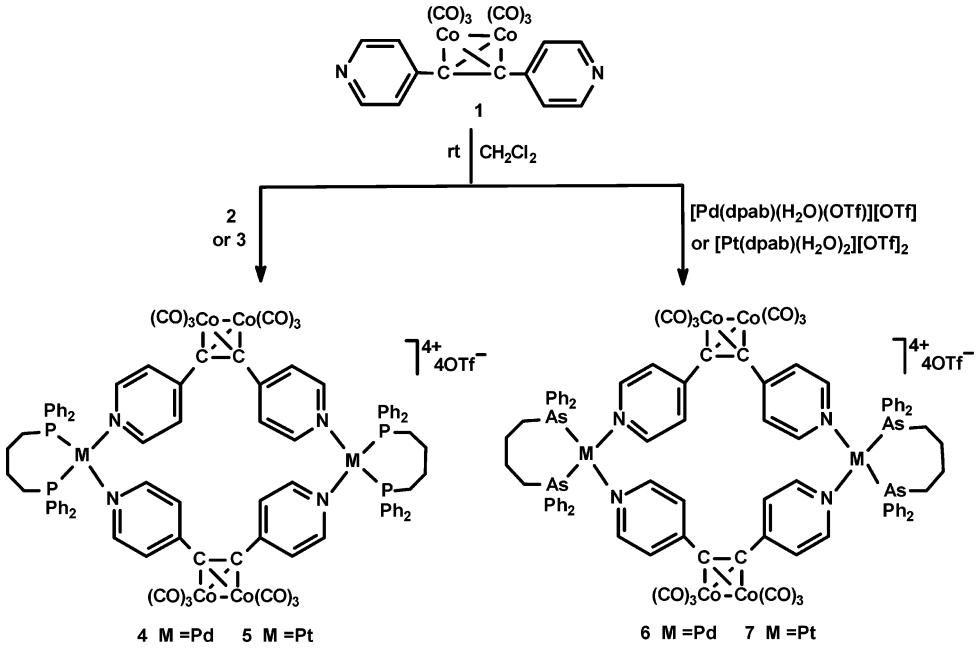

In addition, the Co(1)−Co(2)−Co(1A)−Co(2A) plane in each of **4**−**7** is almost perpendicular (dihedral angles 90.6° and 91.7°) to the plane defined by two Pd or two Pt atoms and four carbon atoms in the two C_2Co_2 cluster cores, whereas the dihedral angles between each of the four pyridine rings in each of **4**−**7** and the defined plane are in the range 72.0−82.5°. It follows that the cationic macrocycles of **4**−**7** are basically isostructural, similar to those cationic macrocycles self-assembled from the flexible C_2Co_2 cluster-bridged bibyridine ligand $(4\text{-}C_5H_4NCO_2CH_2)_2C_2Co_2(CO)_6$. However, in contrast to the macrocycles prepared from the flexible bipyridine ligand, the two pyridine rings of ligand **1** in **4**−**7** are trans to the $Co_2(CO)_6$ moiety and thus the two $Co_2(CO)_6$ moieties lie outside the macrocyclic rings. Interestingly, macrocycles **4**−**7** can be regarded as the first examples of a special type of molecular squares in which two centers of the two tetrahedral C_2Co_2 cluster cores and two Pd or two Pt metal atoms occupy the four corners of the squares, respectively.

Finally, it is worthy of note that the cationic macrocyclic squares of **4**−**7** are stacked at a distance of ca. 13.9 Å between the two nearest transition metal centers of adjacent molecules, which forms channels with a cavity of ca. 7.35 × 7.36 Å; the triflate anions and the solvent molecules included in crystals of **4**−**7** lie between the stacked interlayers.

Electrochemical Study on Ligand $(4\text{-}C_5H_4N)_2C_2Co_2(CO)_6$ (1) and Macrocycles $\{[Pd(dppb)]\text{-}\mu\text{-}[(4\text{-}C_5H_4N)_2C_2Co_2(CO)_6]\}_2[OTf]_4$ (4) and $\{[Pt(dpab)]\text{-}\mu\text{-}[(4\text{-}C_5H_4N)_2C_2Co_2(CO)_6]\}_2[OTf]_4$ (7). The cyclic voltammetric behavior of ligand **1** at different temperatures is presented in Figure 7. As shown in Figure 7a, **1** displays an irreversible reduction peak at −1.49 V, a quasi-reversible reduction peak at −1.78 V, and an irreversible oxidation peak at −0.43 V, respectively. The irreversible peak at −1.49 V in comparison with those displayed by complexes $RC_2R'Co_2(CO)_6$[13−15] should be attributed to the one-electron reduction of the $C_2Co_2(CO)_6$ cluster to give the radical anion of **1**. This radical

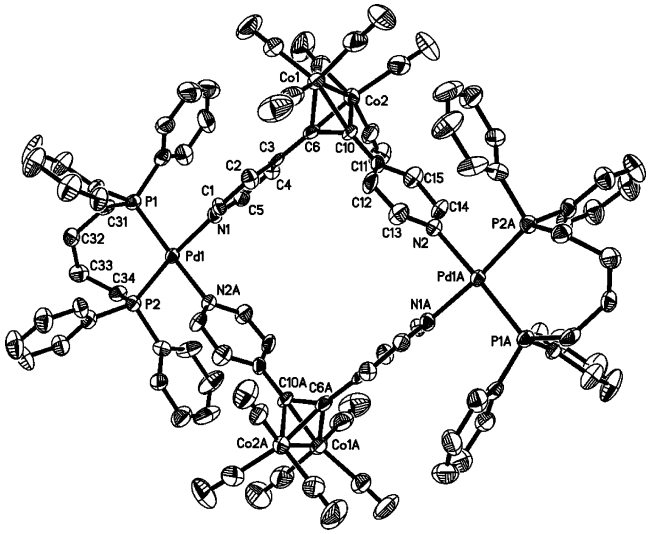

Figure 3. Molecular structure of complex **4**.

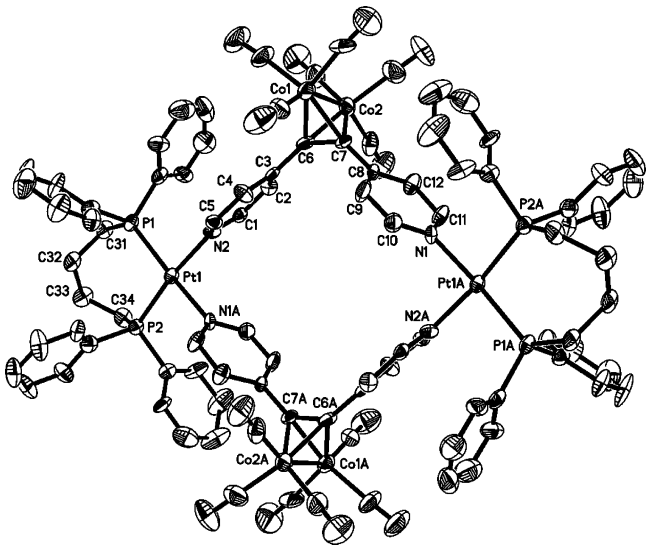

Figure 4. Molecular structure of complex **5**.

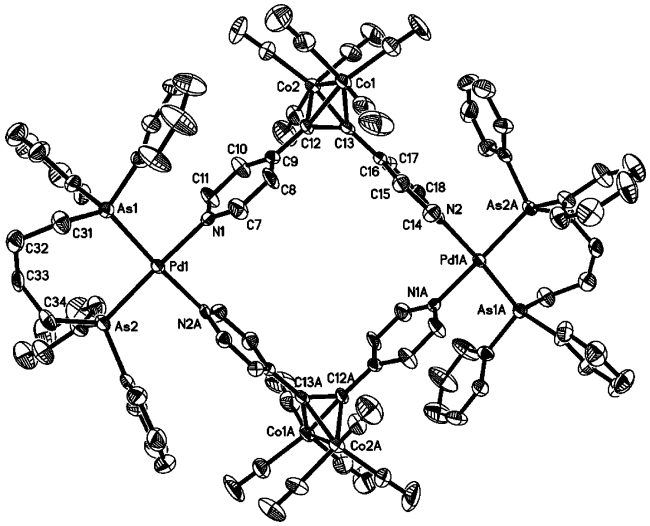

Figure 5. Molecular structure of complex **6**.

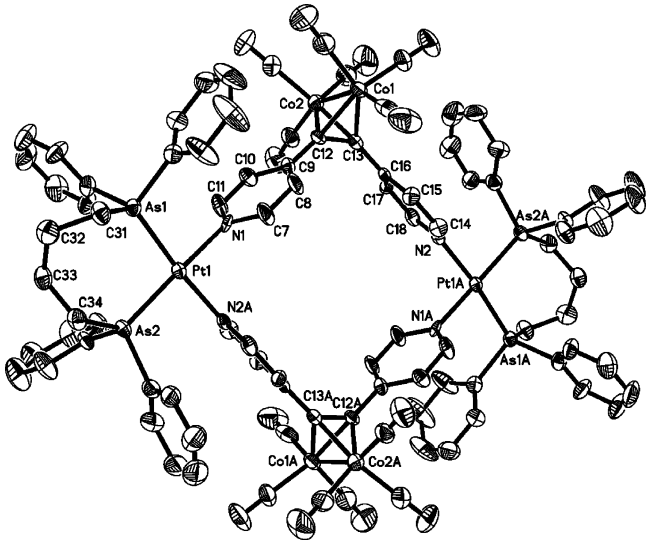

Figure 6. Molecular structure of complex **7**.

Table 3. Selected Bond Lengths (Å) and Angles (deg) for 4

Pd(1)−N(1)	2.095(5)	Pd(1)−N(2A)	2.096(5)
Pd(1)−P(2)	2.2869(19)	Pd(1)−P(1)	2.2901(19)
Co(1)−Co(2)	2.4725(17)	N(1)−C(1)	1.334(7)
C(6)−C(10)	1.374(8)	C(6)−Co(2)	1.956(7)
C(6)−Co(1)	1.974(7)	C(10)−Co(1)	1.975(7)
C(31)−P(1)	1.791(6)	C(34)−P(2)	1.846(6)
N(1)−Pd(1)−N(2A)	86.1(2)	N(1)−Pd(1)−P(2)	173.50(16)
N(2A)−Pd(1)−P(2)	89.23(15)	N(1)−Pd(1)−P(1)	89.39(15)
C(6)−C(10)−Co(1)	69.6(4)	P(2)−Pd(1)−P(1)	95.68(7)
C(6)−Co(1)−C(10)	40.7(2)	Co(2)−C(10)−Co(1)	77.7(2)
C(6)−Co(1)−Co(2)	50.7(2)	C(3)−C(6)−Co(2)	137.0(5)
C(10)−C(6)−C(3)	139.9(6)	C(5)−N(1)−C(1)	116.9(6)

anion is rather unstable and may undergo decomposition on the electrode surface to give the monoanion $Co(CO)_4^-$ with an irreversible one-electron oxidation peak at −0.43 V.[13,14,16] However, in contrast to Figure 7a, Figure 7b shows that the irreversible reduction peak

(13) Arewgoda, M.; Rieger, P. H.; Robinson, B. H.; Simpson, J.; Visco, S. J. *J. Am. Chem. Soc*. **1982**, *104*, 5633.
(14) Osella, D.; Fiedler, J. *Organometallics* **1992**, *11*, 3875.
(15) Osella, D.; Milone, L.; Nervi, C.; Ravera, M. *Eur. J. Inorg. Chem*. **1998**, 1473.
(16) Casagrande, L. V.; Chen, T.; Rieger, P. H.; Robinson, B. H. *Inorg. Chem*. **1984**, *23*, 2019.

Table 4. Selected Bond Lengths (Å) and Angles (deg) for 5

Pt(1)−N(2)	2.080(7)	Pt(1)−N(1A)	2.093(6)
Pt(1)−P(2)	2.269(2)	Pt(1)−P(1)	2.277(2)
Co(1)−Co(2)	2.457(2)	C(6)−C(7)	1.372(10)
C(6)−Co(1)	1.966(9)	C(34)−P(2)	1.864(8)
C(7)−Co(1)	1.949(8)	C(31)−P(1)	1.803(7)
C(6)−Co(2)	1.935(9)	N(2)−C(1)	1.319(9)
N(2)−Pt(1)−N(1A)	85.7(2)	N(2)−Pt(1)−P(2)	172.7(2)
N(1A)−Pt(1)−P(2)	89.17(19)	N(2)−Pt(1)−P(1)	88.54(19)
N(1A)−Pt(1)−P(1)	172.0(2)	P(2)−Pt(1)−P(1)	97.02(9)
C(7)−C(6)−Co(1)	68.8(5)	C(7)−Co(1)−C(6)	41.0(3)
Co(2)−C(6)−Co(1)	78.1(3)	C(7)−Co(1)−Co(2)	50.9(3)
C(10)−N(1)−C(11)	119.1(7)	C(7)−C(6)−C(3)	138.6(8)

Table 5. Selected Bond Lengths (Å) and Angles (deg) for 6

Pd(1)−N(2A)	2.085(7)	Pd(1)−N(1)	2.096(7)
Pd(1)−As(2)	2.3784(12)	Pd(1)−As(1)	2.3852(12)
C(12)−C(13)	1.356(12)	Co(1)−Co(2)	2.471(3)
Co(1)−C(12)	1.960(9)	Co(1)−C(13)	1.954(9)
C(9)−C(12)	1.464(12)	N(1)−C(7)	1.315(12)
As(1)−C(31)	1.962(10)	As(2)−C(34)	1.961(9)
N(2A)−Pd(1)−N(1)	87.5(2)	C(12)−Co(2)−C(13)	40.6(4)
N(1)−Pd(1)−As(2)	175.12(18)	C(13)−Co(1)−Co(2)	50.9(3)
N(1)−Pd(1)−As(1)	89.13(17)	Co(2)−C(12)−Co(1)	78.5(4)
As(2)−Pd(1)−As(1)	94.28(4)	C(9)−C(12)−Co(2)	134.4(7)
N(2A−Pd(1)−As(2)	89.28(18)	C(7)−N(1)−C(11)	117.2(9)

Table 6. Selected Bond Lengths (Å) and Angles (deg) for 7

Pt(1)−N(2A)	2.100(7)	Pt(1)−N(1)	2.103(7)
Pt(1)−As(2)	2.3677(12)	Pt(1)−As(1)	2.3727(12)
C(12)−C(13)	1.360(13)	Co(1)−Co(2)	2.474(3)
C(9)−C(12)	1.444(13)	As(2)−C(34)	1.929(10)
Co(1)−C(12)	1.948(10)	Co(1)−C(13)	1.954(10)
As(1)−C(31)	1.939(10)	N(1)−C(7)	1.339(12)
N(2A)−Pt(1)−N(1)	87.8(3)	C(12)−Co(1)−Co(2)	51.0(3)
N(1)−Pt(1)−As(2)	174.5(2)	C(12)−Co(1)−C(13)	40.8(4)
N(1)−Pt(1)−As(1)	88.24(19)	C(9)−C(12)−Co(2)	135.1(8)
As(2)−Pt(1)−As(1)	95.15(4)	Co(1)−C(12)−Co(2)	78.5(4)
N(2A)−Pt(1)−As(2)	89.13(19)	C(11)−N(1)−C(7)	119.6(8)

at −1.49 V becomes reversible and the irreversible oxidation peak at −0.43 V has disappeared, both implying that the radical anion of **1** seems to be stable at low temperature, −40 ± 1 °C. Apparently, the small reduction peak at −1.78 V in Figure 7a might be due to some unknown species generated directly or indirectly from decomposition of the radical anion of **1**, since this peak has also disappeared in Figure 7b.

The cyclic voltammogram of macrocyclic Pd complex **4** determined at room temperature is shown in Figure

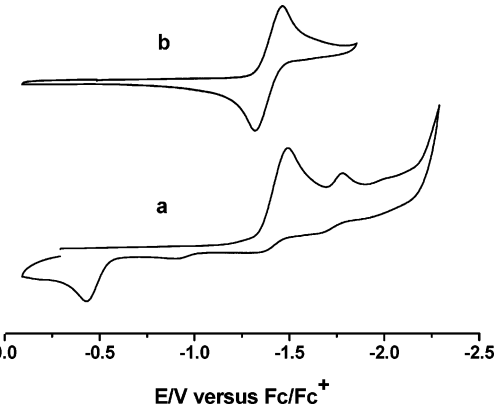

Figure 7. Cyclic voltammgrams of **1** (1 mM) in 0.1 M n-Bu_4NPF_6/CH_2Cl_2. Scan rate 100 mV·s^{-1}. (a) $T = 25 \pm 1$ °C, (b) $T = -40 \pm 1$ °C.

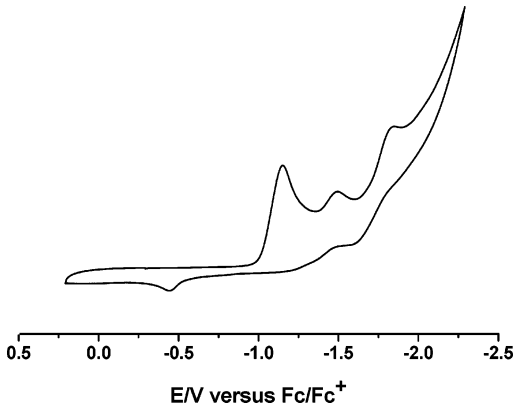

Figure 8. Cyclic voltammgrams of **4** (1 mM) in 0.1 M n-Bu_4NPF_6/CH_2Cl_2. Scan rate 100 mV·s^{-1}. $T = 25 \pm 1$ °C.

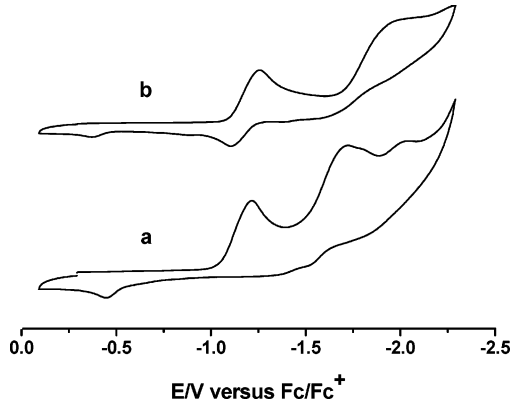

Figure 9. Cyclic voltammgrams of **7** (1 mM) in 0.1 M n-Bu_4NPF_6/CH_2Cl_2. Scan rate 100 mV·s^{-1}. (a) $T = 25 \pm 1$ °C. (b) $T = -40 \pm 1$ °C.

8. As illustrated in Figure 8, this complex undergoes an irreversible reduction at −1.15 V, two quasi-reversible reductions at −1.49 and −1.85 V, and an irreversible oxidation at −0.44 V. The reduction peak at −1.15 V could be attributed not only to the one-electron reduction of Pd(II)[17] but also to that of the $C_2Co_2(CO)_6$ cluster in **4**. This is because the reduction peak is much higher than that for only Pd(II) and the reduction of the $C_2Co_2(CO)_6$ cluster in cationic macrocycle **4** should be expected to occur in a much more positive direction when compared to the reduction of the $C_2Co_2(CO)_6$ cluster in free ligand **1** at −1.49 V described above. While the second reduction peak at −1.49 V is due to the one-electron reduction of free ligand **1** released from **4**, the third peak at −1.85 V might be possibly owing to the one-electron reduction of Pd(I).[17] Just like in Figure 7a, the irreversible peak at −0.44 V should be attributed to the one-electron oxidation of monoanion $Co(CO)_4^-$ generated in situ during the electrochemical process.[13,14,16]

Figure 9 compares the cyclic voltammetric behavior of macrocyclic Pt complex **7** at different temperatures. As shown in Figure 9a, complex **7** occurs in two irreversible reductions at −1.22 and −1.72 V and an irreversible oxidation at −0.44 V at room temperature. Similar to **4**, these three peaks displayed by **7** could be reasonably attributed to the one-electron reduction of its $C_2Co_2(CO)_6$ cluster,[13−15] transition metal Pt(II),[17,18] and the $Co(CO)_4^-$ monoanion generated during the electrochemical determinations,[14,16] respectively. The small irreversible reduction peak at −2.04 V in Figure 9a might be caused by some unknown decomposition species produced at room temperature. In fact, this reduction peak along with the oxidation peak at −0.44 V have basically disappeared in its low-temperature cyclic voltammogram (Figure 9b).

Conclusions

The tetrahedral C_2Co_2 cluster-containing metallomacrocycles **4**−**7**, which represent a special type of molecular squares, have been synthesized by self-assembly of the rigid C_2Co_2 cluster-bridged bipyridine ligand **1** with the dppb-chelated Pd(II)/Pt(II) complexes **2** and **3** or the dpab-chelated Pd(II)/Pt(II) complexes [Pd(dpab)-(H_2O)(OTf)][OTf] and [Pd(dpab)$(H_2O)_2$][OTf]$_2$, respectively. While the structures of new complexes **1**−**7** were characterized, the cyclic voltammetric properties of **1**, **4**, and **7** were investigated. Interestingly, the cyclic voltammetric behavior of **1** and **7** has been demonstrated to be dependent upon the temperature. For example, the irreversible reduction peak of **1** at −1.49 V or that of **7** at −1.22 V displayed at room temperature becomes reversible at low temperature, -40 ± 1 °C. All the redox peaks for **1**, **4**, and **7** have been preliminarily assigned, and the reasons for such a temperature-dependent behavior are discussed. Particularly interesting is that the ready availability of both flexible and rigid C_2Co_2 cluster-bridged ligands (4-$C_5H_4NCO_2CH_2)_2C_2$-$Co_2(CO)_6$[8] and **1** should make it possible to further compare their chemical behavior in self-assembly with other transition metals and to prepare different types of C_2Co_2 cluster-containing metallomacrocycles that may have novel properties due to incorporation of the tetrahedral C_2Co_2 cluster[19] into a variety of metallomacrocycles.

Experimental Section

General Comments. All reactions were carried out under an atmosphere of highly purified nitrogen using standard Schlenk or vacuum-line techniques. Solvents for preparative use were dried and distilled under nitrogen from CaH_2 or sodium/benzophenone ketyl prior to use. Silver triflate and $Co_2(CO)_8$ were of commercial origin and used as purchased. Pd(dppb)Cl_2,[20] Pt(dppb)Cl_2,[9] [Pd(dpab)(H_2O)(OTf)][OTf],[8] [Pd(dpab)$(H_2O)_2$][OTf]$_2$[8] and bis(4-pyridyl)acetylene[21] were prepared according to literature methods. ^{1}H NMR spectra were recorded on a Bruker AC-P 200 or a Bruker 300M NMR spectrometer. ^{19}F NMR spectra were measured on a Bruker 400M spectrometer, and chemical shifts are referenced relative to external $CFCl_3$ ($\delta = 0$). ^{31}P NMR spectra were taken on a Bruker AC-P 200 or a Bruker 300 M NMR spectrometer, and chemical shifts are reported in ppm relative to external 85% H_3PO_4. IR spectra were taken on a Bio-Rad FTS 135 spectrophotometer. Elemental analysis was performed on an Elementar Vario EL analyzer, and melting points were determined on a Yanaco MP-500 melting point apparatus.

Preparation of (4-$C_5H_4N)_2C_2Co_2(CO)_6$ (1). A Schlenk flask was charged with 0.27 g (1.5 mmol) of bis(4-pyridyl)-

(17) Grant, G. J.; Garter, S. M.; Russell, A. L.; Poullaos, I. M.; VanDerveer, D. G. *J. Organomet. Chem.* **2001**, *637−639*, 683.
(18) Granifo, J.; Vargas, M. E.; Garland, M. T.; Baggio, R. *Inorg. Chim. Acta* **2000**, *305*, 143.
(19) Dickson, R. S.; Fraser, P. J. *Adv. Organomet. Chem.* **1974**, *12*, 323.
(20) Parshall, G. W. *Inorg. Synth.* **1970**, *12*, 27.
(21) Tanner, M.; Ludi, A. *Chimia* **1980**, *34*, 23.

Table 7. Crystal Data and Structural Refinement Details for 2 and 3

	2	**3**
mol formula	$C_{30}H_{32}F_6O_8P_2PdS_2 \cdot CH_2Cl_2$	$C_{30}H_{32}F_6O_8P_2PtS_2 \cdot CHCl_3$
mol wt	951.94	1075.07
cryst syst	monoclinic	monoclinic
space group	$P2(1)/n$	$P2(1)/n$
a/Å	11.444(5)	11.515(5)
b/Å	21.805(9)	21.608(9)
c/Å	16.029(7)	16.205(7)
α/deg	90	90
β/deg	91.686(7)	93.602(6)
γ/deg	90°	90
V/Å^3	3998(3)	4024(3)
Z	4	4
D_c/g·cm^{-3}	1.581	1.775
abs coeff/mm^{-1}	0.855	3.943
cryst size/mm	0.30 × 0.25 × 0.20	0.20 × 0.12 × 0.09
F(000)	1920	2112
$2\theta_{max}$/deg	41.64	53.00
no. of reflns	10 305	22 566
no. of indep reflns	4183 (R_{int} = 0.0253)	8277 (R_{int} = 0.0398)
index ranges	$-11 \le h \le 10$ $-21 \le k \le 15$ $-16 \le l \le 16$	$-14 \le h \le 13$ $-17 \le k \le 27$ $-20 \le l \le 20$
scan type	$\omega-2\theta$	$\omega-2\theta$
no. of data/restraints/params	4183/10/486	8277/24/510
goodness of fit on F^2	1.052	1.063
R	0.0383	0.0456
R_w	0.0821	0.1158
largest diff peak and hole/e Å^{-3}	0.662/−0.617	1.074/−0.957

Table 8. Crystal Data and Structural Refinement Details for 4−7

	4	**5**	**6**	**7**
mol formula	$C_{96}H_{72}Co_4F_{12}N_4O_{24}P_4Pd_2S_4 \cdot 6CHCl_3$	$C_{96}H_{72}Co_4F_{12}N_4O_{24}P_4Pt_2S_4 \cdot 6CHCl_3$	$C_{96}H_{72}As_4Co_4F_{12}N_4O_{24}Pd_2S_4 \cdot 8CHCl_3$	$C_{96}H_{72}As_4Co_4F_{12}N_4O_{24}Pt_2S_4 \cdot 8CHCl_3$
mol wt	3310.42	3487.80	3724.96	3902.34
cryst syst	triclinic	triclinic	triclinic	triclinic
space group	$P\bar{1}$	$P\bar{1}$	$P\bar{1}$	$P\bar{1}$
a/Å	13.871(5)	13.813(6)	13.947(4)	13.927(5)
b/Å	16.717(6)	16.650(7)	17.222(5)	16.983(6)
c/Å	18.592(6)	18.558(8)	18.691(5)	18.688(7)
α/deg	113.802(5)	113.828(6)	113.761(4)	113.920(6)
β/deg	102.796(6)	102.927(7)	102.740(4)	102.869(6)
γ/deg	96.690(6)	96.944(7)	97.570(4)	97.178(7)
V/Å^3	3743(2)	3697(3)	3883.2(19)	3822(2)
Z	1	1	1	1
D_c/g·cm^{-3}	1.469	1.567	1.593	1.695
abs coeff/mm^{-1}	1.160	2.822	2.028	3.653
cryst size/mm	0.16 × 0.12 × 0.09	0.24 × 0.17 × 0.12	0.26 × 0.22 × 0.20	0.32 × 0.30 × 0.22
F(000)	1648	1712	1836	1900
$2\theta_{max}$/deg	51.00	51.00	52.92	52.96
no. of reflns	19 569	19 316	22 391	22 289
no. of indep reflns	13 566 (R_{int} = 0.0698)	13 482 (R_{int} = 0.0682)	15 787 (R_{int} = 0.0450)	15 529 (R_{int} = 0.0493)
index ranges	$-13 \le h \le 16$ $-17 \le k \le 20$ $-22 \le l \le 21$	$-11 \le h \le 16$ $-20 \le k \le 20$ $-22 \le l \le 15$	$-17 \le h \le 17$ $-21 \le k \le 11$ $-21 \le l \le 23$	$-17 \le h \le 17$ $-21 \le k \le 19$ $-16 \le l \le 23$
scan type	$\omega-2\theta$	$\omega-2\theta$	$\omega-2\theta$	$\omega-2\theta$
no. of data/restraints/params	13 566/0/784	13 482/0/784	15 787/170/911	15 529/200/911
goodness of fit on F^2	0.811	0.876	0.996	0.969
R	0.0672	0.0629	0.0724	0.0611
R_w	0.1069	0.1071	0.1927	0.1445
largest diff peak and hole/e Å^{-3}	0.696/−0.441	1.949/−1.425	1.334/−0.726	1.629/−1.448

acetylene, 5 mL of CH_2Cl_2, and 25 mL of petroleum ether. While stirring, a solution of 0.514 g (1.5 mmol) of $Co_2(CO)_8$ in 15 mL of petroleum ether was slowly added. The mixture was stirred at room temperature for 2−3 h until no CO evolution was observed. Solvent was removed under reduced pressure, and the residue was subjected to filtration chromatography using acetone as eluent. Removal of the solvent from the eluted red band gave 0.425 g (61%) of **1** as a crystalline dark red solid, mp 93 °C dec. Anal. Calcd for $C_{18}H_8Co_2N_2O_6$: C, 46.38; H, 1.73; N, 6.01. Found: C, 46.39; H, 1.71; N, 6.02. IR (KBr disk): $\nu_{C\equiv O}$ 2093 (s), 2066 (vs), 2043 (s), 2024 (vs), 2004 (s) cm^{-1}. ^{1}H NMR (200 MHz, $CDCl_3$): δ 8.60 (d, J = 5.8 Hz, 4H, 4H$_\alpha$), 7.34 (d, J = 5.2 Hz, 4H, 4H$_\beta$). ^{13}C NMR (50.3 MHz, $CDCl_3$): δ 198.14 (C≡O), 150.57 (C$_\alpha$), 147.00 (C$_\gamma$), 123.55 (C$_\beta$), 87.98(CCo).

[Pd(dppb)(H$_2$O)$_2$][OTf]$_2$·CH$_2$Cl$_2$ (2). To a suspension of 0.192 g (0.32 mmol) of Pd(dppb)Cl_2 in 30 mL of CH_2Cl_2 was added 0.205 g (0.80 mmol) of AgOTf. The reaction mixture was stirred at room temperature for 24 h with the exclusion of light. The resulting mixture was filtered in air, and the filtrate was concentrated to ca. 2 mL under reduced pressure. Diethyl ether was added to give a precipitate, and the precipitate was washed with diethyl ether, dried in a vacuum to give 0.292 g

(96%) of **2** as a light yellow solid, mp 175 °C dec. Anal. Calcd for $C_{31}H_{34}Cl_2F_6O_8P_2PdS_2$: C, 39.11; H, 3.60. Found: C, 39.36; H, 3.89. IR (KBr disk): ν_{OH} 3221 (m); ν_{OTf} 1289 (vs), 1248 (vs), 1177 (s), 1102 (s), 1029 (vs) cm^{-1}. ^1H NMR (200 MHz, $CDCl_3$): δ 7.61−7.24 (m, 20H, $4C_6H_5$), 5.28 (s, 2H, CH_2Cl_2), 4.98 (br s, 4H, $2H_2O$), 2.61 (s, 4H, $2CH_2P$), 2.03 (s, 4H, $2CH_2$). ^{31}P NMR (81 MHz, $CDCl_3$): δ 35.18 (s, 2P). ^{19}F NMR (376 MHz, $CDCl_3$): δ −79.15 (s, $2SO_3CF_3$).

[Pt(dppb)(H$_2$O)$_2$][OTf]$_2$ (3). By a procedure similar to that described in the preparation of **2**, 0.151 g (94%) of **3** was obtained as a white solid from 0.117 g (0.169 mmol) of $Pt(dppb)Cl_2$, 0.130 g (0.506 mmol) of AgOTf, and 25 mL of CH_2Cl_2, mp 122−124 °C. Anal. Calcd for $C_{30}H_{32}F_6O_8P_2PtS_2$: C, 37.70; H, 3.37. Found: C, 37.68; H, 3.32. IR (KBr disk): ν_{OH} 3056 (m); ν_{OTf} 1289 (vs), 1253 (vs), 1172 (s), 1102 (s), 1032 (vs) cm^{-1}. ^1H NMR (200 MHz, $CDCl_3$): δ 7.64−7.42 (m, 20H, $4C_6H_5$), 2.84 (br s, 4H, $2H_2O$), 2.63 (s, 4H, $2CH_2P$), 2.03 (s, 4H, $2CH_2$). ^{31}P NMR (81 MHz, acetone-d_6): δ 10.47 (t, J_{Pt-P} = 1761 Hz, 2P). ^{19}F NMR (376 MHz, $CDCl_3$): δ −78.90 (s, $2SO_3CF_3$).

[Pd(dppb)]-μ-[(4-C$_5$H$_4$N)$_2$C$_2$Co$_2$(CO)$_6$]$_2$[OTf]$_4$ (4). A Schlenk flask was charged with 0.048 g (0.05 mmol) of $[Pd(dppb)(H_2O)_2][OTf]_2$, 0.023 g (0.05 mmol) of $(4\text{-}C_5H_4N)_2C_2Co_2(CO)_6$, and 10 mL of CH_2Cl_2. The mixture was stirred at room temperature for 2−3 h, and the resulting mixture was filtered. The filtrate was condensed to ca. 2 mL under reduced pressure. Diethyl ether was added to give a precipitate, which was washed with diethyl ether and dried in vacuo to produce 0.040 g (62%) of **5** as a red solid, mp 98 °C dec. Anal. Calcd for $C_{96}H_{72}Co_4F_{12}N_4O_{24}$ $P_4Pd_2S_4$: C, 44.45; H, 2.80; N, 2.16. Found: C, 44.26; H, 3.08; N, 2.18. IR (KBr disk): $\nu_{C\equiv O}$ 2105 (vs), 2070 (vs), 2051 (vs); ν_{OTf} 1257 (vs), 1224 (s), 1156 (s), 1030 (vs) cm^{-1}. ^1H NMR (300 MHz, $CDCl_3$): δ 8.52 (d, J = 5.1 Hz, 8H, $8H_\alpha$), 7.71−7.46 (m, 40H, $8C_6H_5$), 6.77 (d, J = 5.7 Hz, 8H, $8H_\beta$), 3.19 (br s, 8H, $4CH_2P$), 1.78 (br s, 8H, $4CH_2$). ^{31}P NMR (121 MHz, $CDCl_3$): δ 26.70 (s, 4P). ^{19}F NMR (376 MHz, $CDCl_3$): δ −78.62 (s, $4SO_3CF_3$).

[Pt(dppb)]-μ-[(4-C$_5$H$_4$N)$_2$C$_2$Co$_2$(CO)$_6$]$_2$[OTf]$_4$ (5). In a manner similar to that described in the preparation of **4**, 0.045 g (65%) of **5** was obtained as a red solid from 0.048 g (0.05 mmol) of $[Pt(dppb)(H_2O)_2][OTf]_2$ and 0.023 g (0.05 mmol) of $(4\text{-}C_5H_4N)_2C_2Co_2(CO)_6$, mp 103 °C dec. Anal. Calcd for $C_{96}H_{72}Co_4F_{12}N_4O_{24}P_4Pt_2S_4$: C, 41.60; H, 2.62; N, 2.02. Found: C, 41.69; H, 2.66; N, 1.99. IR (KBr disk): $\nu_{C\equiv O}$ 2105 (s), 2070 (vs), 2046 (vs); ν_{OTf} 1260 (vs), 1224 (s), 1156 (s), 1030 (vs) cm^{-1}. ^1H NMR (300 MHz, $CDCl_3$): δ 8.54 (d, J = 5.4 Hz, 8H, $8H_\alpha$), 7.74−7.46 (m, 40H, $8C_6H_5$), 6.79 (d, J = 5.1 Hz, 8H, $8H_\beta$), 3.28 (br s, 8H, $4CH_2P$), 1.70 (br s, 8H, $4CH_2$). ^{31}P NMR (121 MHz, $CDCl_3$): δ 2.08 (t, J_{Pt-P} = 1583 Hz, 4P). ^{19}F NMR (376 MHz, $CDCl_3$): δ −78.78 (s, $4SO_3CF_3$).

[Pd(dpab)]-μ-[(4-C$_5$H$_4$N)$_2$C$_2$Co$_2$(CO)$_6$]$_2$[OTf]$_4$ (6). By a procedure similar to that described in the preparation of **4**, 0.055 g (79%) of **6** was obtained as a red solid from 0.047 g (0.05 mmol) of $[Pd(dpab)(H_2O)(OTf)][OTf]$ and 0.023 g (0.05 mmol) of $(4\text{-}C_5H_4N)_2C_2Co_2(CO)_6$, mp 100 °C dec. Anal. Calcd for $C_{96}H_{72}As_4Co_4F_{12}N_4O_{24}Pd_2S_4$: C, 41.62; H, 2.62; N, 2.02. Found: C, 41.65; H, 2.68; N, 2.13. IR (KBr disk): $\nu_{C\equiv O}$ 2105 (s), 2070 (vs), 2051 (vs); ν_{OTf} 1256 (vs), 1223 (s), 1158 (s), 1030 (vs) cm^{-1}. ^1H NMR (300 MHz, $CDCl_3$): δ 8.70 (d, J = 6.03 Hz, 8H, $8H_\alpha$), 7.60−7.39 (m, 40H, $8C_6H_5$), 6.73 (d, J = 6.03 Hz, 8H, $8H_\beta$), 3.26 (br.s, 8H, $4CH_2As$), 1.77 (br s, 8H, $4CH_2$). ^{19}F NMR (376 MHz, $CDCl_3$): δ −78.69 (s, $4SO_3CF_3$).

[Pt(dpab)]-μ-[(4-C$_5$H$_4$N)$_2$C$_2$Co$_2$(CO)$_6$]$_2$[OTf]$_4$ (7). In a manner similar to that described in the preparation of **4**, 0.050 g (68%) of **7** was obtained as a red solid from 0.052 g (0.05 mmol) of $[Pt(dpab)(H_2O)_2][OTf]_2$ and 0.023 g (0.05 mmol) of $(4\text{-}C_5H_4N)_2C_2Co_2(CO)_6$, mp 97 °C dec. Anal. Calcd for $C_{96}H_{72}As_4Co_4F_{12}N_4O_{24}Pt_2S_4$: C, 39.12; H, 2.46; N, 1.90. Found: C, 39.15; H, 2.46; N, 2.03. IR (KBr disk): $\nu_{C\equiv O}$ 2105 (s), 2070 (vs), 2044 (vs); ν_{OTf} 1259 (vs), 1224 (s), 1156 (s), 1030 (vs) cm^{-1}. ^1H NMR (300 MHz, $CDCl_3$): δ 8.78 (d, J = 6.0 Hz, 8H, $8H_\alpha$), 7.68−7.41 (m, 40H, $8C_6H_5$), 6.79 (d, J = 6.0 Hz, 8H, $8H_\beta$), 3.31 (br s, 8H, $4CH_2As$), 1.74 (br s, 8H, $4CH_2$). ^{19}F NMR (376 MHz, $CDCl_3$): δ −78.76 (s, $4SO_3CF_3$).

X-ray Structure Determinations of 2−7. X-ray quality single crystals of **2** and **3** were grown by slow diffusion of diethyl ether or *n*-hexane into their CH_2Cl_2 solutions at room temperature, whereas single crystals of **4**−**7** were obtained from their chloroform solutions at −20 °C. It is worth pointing out that the single crystals of **4**−**7** must be sealed in a capillary as soon as they are taken out from their mother liquors, since the single crystals of **4**−**7** easily collapse into amorphous materials due to loss of their solvent molecules. Each single crystal suitable for X-ray diffraction analysis was mounted on a Bruker SMART-1000 CCD area detector diffractometer. Data were collected at 293(2) K using graphite-monochromated Mo Kα radiation (λ = 0.71073 Å) in the ω scanning mode. Absorption corrections were performed using SADABS. The structures were solved by direct methods using the SHELXS-97 program[22] and refined by full-matrix least-squares techniques (SHELXL-97)[23] on F^2. All hydrogen atoms were located by using the geometric method. Details of the crystal data, data collections, and structure refinements are summarized in Tables 7 and 8, respectively.

Electrochemical Determinations of 1, 4, and 7. Cyclic voltammograms of **1**, **4**, and **7** were obtained on a BAS Epsilon potentiostat using a standard three-electrode system consisting of a glassy-carbon working electrode (3 mm in diameter), an Ag/Ag^+ (0.01 M $AgNO_3$/0.1 M *n*-Bu_4NPF_6 in CH_3CN) reference electrode, and a Pt-wire auxiliary electrode. A solution of 0.1 M *n*-Bu_4NPF_6 in CH_2Cl_2 (HPLC grade) was used as supporting electrolyte.The working electrode was polished with 0.05 μm alumina and sonicated in water for 10 min prior to use. All solutions were deoxygenated with nitrogen for at least 10 min prior to use. All potentials are quoted against the ferrocene/ferrocenium (Fc/Fc^+) potential.

Acknowledgment. We are grateful to the National Natural Science Foundation of China and the Research Fund for the Doctoral Program of Higher Education of China for financial support.

Supporting Information Available: All crystal data, atomic coordinates, thermal parameters, and bond lengths and angles for **2**−**7** in CIF format. This material is available free of charge via the Internet at http://pubs. acs.org.

OM050668S

(22) Sheldrick, G. M. *SHELXS97*, A Program for Crystal Structure Solution; University of Göttingen, Germany, 1997.

(23) Sheldrick, G. M. *SHELXL97*, A Program for Crystal Structure Refinement; University of Göttingen, Germany, 1997.